Express Polymer Letters Vol.18, No.1 (2024) 41–60
Available online at www.expresspolymlett.com
https://doi.org/10.3144/expresspolymlett.2024.4

Research article

Damage assessment through cyclic load-unload tensile tests for ply-level hybrid carbon fiber composites

Maria Casapu[1,2,3*], *Ion Fuiorea*[1], *Michel Arrigoni*[2]

[1]University Politehnica of Bucharest, 313 Splaiul Independenței, Sector 6, 060042 Bucharest, Romania
[2]ENSTA Bretagne, IRDL, UMR CNRS 6027, 2 rue François VERNY, 29806 Brest Cedex 09, France
[3]Military Technical Academy 'Ferdinand I', 39–49 George Cosbuc Avenue, Sector 5, 050141 Bucharest, Romania

Received 27 July 2023; accepted in revised form 29 September 2023

Abstract. Composite materials are of increasing interest in aircraft and spacecraft structures, and carbon fiber reinforced polymers (CFRP) have emerged as materials meeting quality standards for structural applications in the aircraft industry. Despite their high mechanical properties, CFRPs are associated with high production costs. Building on recent research by the authors, this paper investigates the use of ply-level hybridization to reduce manufacturing costs while maintaining the mechanical performance of the manufactured material. Focusing on the causes of nonlinear response under off-axis tensile loading, the paper involves cyclic load-unload (LU) tensile tests conducted at off-axis angles of 15°, 30°, and 45° to predict mechanical characteristics and damage evolution. Residual strains are directly extracted from load-unload stress-strain responses. Three distinct methods for estimating cycle modulus are employed and compared for damage variable formulation. The research findings reveal dependencies of both the damage variable and residual strains on the off-axis angle. Furthermore, the method used to assess the modulus during cycling loading significantly influences the damage variable estimation. Encouragingly, the hybrid laminates exhibit reduced internal damage and matrix plasticity compared to reference counterparts, indicating a positive effect on the mechanical performances of hybridized CFRPs in addition to the cost reduction.

Keywords: *hybridization, residual strain, damage variable, mechanical properties, thermoset composites*

1. Introduction

Composite materials, specifically carbon fiber reinforced polymers (CFRP), have become a fundamental material choice for lightweight structural applications, such as spacecraft and aircraft. CFRP is offered in various grades [1], where higher quality grades correspond to enhanced mechanical properties and higher costs. To address cost-effectiveness while preserving technical performance, there has been significant interest in the concept of hybridization [2–4]. The aim is to mitigate costs or reduce the carbon footprint of materials while still maintaining the desired level of technical performance.

Previous research on composite hybridization has extensively studied the effects of glass-carbon fiber hybridization on composite laminates, but fewer studies have investigated all-carbon fiber hybrid composites. Curtis and Browne [2] combined standard-quality carbon fiber plies with ultra-high-performance carbon fibers, achieving a similar mechanical response to composites made solely with ultra-high-performance fibers and reducing costs by 17%. Naito *et al.* [5] combined high strength with high-modulus carbon fibers, resulting in an intermediate initial modulus and a complicated stress-strain response. Czél *et al.* [6] employed all-carbon hybridization to obtain a pseudo-ductile failure response by blocking low-strain to-failure carbon fibers with high and ultra-high modulus fibers. Dransfeld *et al.* [7] achieved pseudo-ductility in a quasi-isotropic hybrid

*Corresponding author, e-mail: maria.demsa@mta.ro

laminate with carbon fibers of different elastic moduli. Furtado *et al.* [8] introduced ply-level hybridization by mixing prepregs with different ply thicknesses, improving the notched response of thin-ply composites. Sebaey and Mahdi [9] and Sasikumar *et al.* [10] investigated ply-level hybridization for compression after impact (CAI) strength improvement. However, no studies have examined the response of all-carbon hybrid composites under high-velocity impact and high-strain loading. Furthermore, the mentioned works primarily used a quasi-isotropic layup, and there is limited research on the effects of ply-level hybridization in unidirectional (UD) composites. Amacher *et al.* [11] studied the effect of ply thickness on the mechanical response of unidirectional and quasi-isotropic carbon fiber laminates and found no significant difference in properties between different ply thicknesses within the same prepreg system. The previously mentioned studies achieved hybridization by varying either the thickness of the plies or the type of carbon fiber. In this study, the objective is to achieve hybridization by incorporating variations in ply thickness as well as carbon fiber type and analyze the effects. Unidirectional laminates were selected as the focus of this study to gain a fundamental understanding of the impact of hybridization.

As observed in a previous study [12], the stress-strain response of unidirectional carbon fiber composites, whether they are hybrid or not, shows a nonlinear shape when loaded off-axis. Various studies have investigated the nonlinear behavior of composite laminates and its implications. Hahn and Tsai [13] conducted experiments and developed analytical models to understand the effect of nonlinear constituent laminae on laminate behavior. Ogihara [14] studied the nonlinear response of the T300/2500 carbon/epoxy system under off-axis tensile loading, observing softening nonlinearity in off-axis specimens. Yokozeki *et al.* [15] explored the nonlinear mechanical behaviors and strengths of CFRP unidirectional and multidirectional laminates under compressive loadings. They used a one-parameter plasticity model combined with nonlinear elasticity to characterize the nonlinear mechanical properties of unidirectional composites. Ma *et al.* [16] examined the off-axis behavior of PEEK/AS4 unidirectional thermoplastic composites, identifying a linear-elastic relationship during the initial stage and non-linear behavior during the strain-hardening phase.

Different models used to predict the nonlinear behavior of unidirectional fiber reinforced composites loaded off-axis attribute the nonlinearity of the response either to plastic deformation of the matrix [17–20], to internal damage and stiffness reduction [21, 22], or both [23–28].

Building upon the groundwork of prior studies [12, 29], this research explores the origins of nonlinear behavior in off-axis tests for the studied unidirectional ply-level hybrid composite materials. In this regard, cyclic load-unload (LU) tests are performed, with the amplitude of the stress level increasing for each cycle. In a previous investigation of the off-axis behavior of ply-level hybrid composites [12], an intriguing finding emerged – ply-level hybrid materials exhibit strain hardening within the non-linear response region, displaying superior stress levels at equivalent strains compared to both types of reference laminates. The damage/plasticity analysis provides a deeper understanding of the factors contributing to this behavior. Moreover, we evaluate the presence or absence of thickness effects in the tested reference laminates, as there is a lack of scientific papers addressing thickness effects in this specific loading scenario and damage assessment.

This research presents a contribution by employing established damage assessment methods found in existing literature while also introducing an application of the regression method for damage analysis purposes. A distinctive aspect of this study is that we have not encountered any prior work in which these methods are applied to the same dataset, allowing us to compare and contrast their outcomes and thus uncover their respective strengths and limitations.

2. Materials and methods

This study focuses on unidirectional carbon fiber-reinforced composites (UD CFRP). Two different prepregs, namely HSC-500-DT102S-40EF (HSC) and UTS-150-DT120-32F (UTS), were used to manufacture the composite laminates. Throughout this paper, these prepregs will be denoted as HSC and UTS prepregs, respectively, in correspondence with the carbon fiber type present in each prepreg. The DT102S is a thermosetting epoxy with a glass transition temperature T_g of 120–130 °C, while the DT120 is a toughened thermosetting epoxy known for its high-impact strength, and has a glass transition temperature T_g of 115–120 °C, provided by the manufacturer's datasheet. Both prepregs are manufactured by Delta-Preg® (Sant'Egidio alla Vibrata, Italy), and the thermosetting resins are produced by Delta-Tech® (Altopascio, Italy) and employ a medium-temperature curing process.

The key distinction between the two prepregs lies in the fibers' quality.

The UTS prepreg incorporates UTS50 standardized carbon fibers manufactured by Teijin Tenax® (Tokyo, Japan), with well-documented mechanical properties that have a longitudinal modulus of 245 GPa and a strength of 5100 MPa. The elongation at break is 2.1%, and the density is 1.78 g/cm^3.

The HSC prepreg employs non-standardized high-strength carbon (HS carbon) fibers, and the prepreg manufacturer provides only the minimum potential values for the mechanical properties of the HS carbon fibers without specifying their manufacturer. For HS carbon fibers, the longitudinal modulus is ≥230 GPa, and the strength is ≥3800 MPa. The elongation at break is between 1.6 and 2.1%, and the density is not specified within the prepreg datasheet.

This difference in fiber quality and standardization also affects the cost/areal weight of the prepregs.

All laminate panels were cured in an autoclave according to the prepreg manufacturer's specifications, and the laminate manufacturing was carried out by Belcoavia S.R.L (Livezile, Romania).

To achieve ply-level hybridization in both ply thickness and material type, for an unsymmetric, thinner laminate denoted as H1 material, a stacking sequence of 2HSC+1UTS+1HSC+1UTS [0°] was employed. For a symmetric, thicker laminate referred to as H2 material, we adopted a stacking sequence of 1HSC+1UTS+2HSC+1UTS+1HSC [0°].

The selection of the stacking sequence for the hybrid laminates was initially determined, and based on the estimated areal weight provided by the UTS prepregs' datasheet (150 g/m^2), the number of plies for the UTS type laminates was chosen to match the areal mass and laminate thickness of H1 and H2 samples as closely as possible. Consequently, laminates consisting of 13 and 17 UTS plies were manufactured and labeled as UTS13 and UTS17, respectively. Since the HSC prepreg utilizes thick plies with a high areal mass (500 g/m^2), the laminates were created by adjusting the number of HSC plies within each type of hybrid laminate. This adjustment aimed to examine whether the mechanical behavior would vary by simply adding two additional UTS plies. The HSC laminates were constructed with 3 and 4 plies and will be referred to as HSC3 and HSC4, respectively.

The stacking sequence of the laminates is described in Table 1, and fiber volume fractions determined in previous work are provided as well [29]. Cross-section views of the described laminates are shown in Figure 1 [12]. The same laminates were used in previous studies [12, 29], in which characterization of internal structure, physical properties, and on and off-axis quasi-static mechanical properties are provided.

3. Experimental setup and specimen description

To investigate the nature of the nonlinear stress-strain response in off-axis tensile tests of the unidirectional carbon-fiber materials from this study, cyclic load-unload tensile tests were performed for off-axis angles of 15°, 30°, and 45°. The number of cycles is limited to a maximum of six to avoid low cycle fatigue phenomenon effects [28], with six cycles being applied for the first two off-axis angles, and four cycles for the last one, as the maximum stress level reached by the was lower than for the other angles.

To choose the unloading stress levels, the monotonic stress-strain response from a previous study [12] was analyzed. The first unloading stress level was chosen as being half the stress at which the nonlinear response begins. The second level was at the stress value where the nonlinear response begins, and for

Table 1. Laminate details of hybridized and non-hybridized CFRP samples.

Laminate name	Stacking sequence	Fiber volume fraction [29] [%]
HSC3	HSC[0°]$_3$	49.84
HSC4	HSC[0°]$_4$	49.31
UTS13	UTS[0°]$_{13}$	54.46
UTS17	UTS[0°]$_{17}$	53.67
H1	2HSC+1UTS+1HSC+1UTS [0°]	50.32
H2	1HSC+1UTS+2HSC+1UTS+1HSC [0°]	52.14

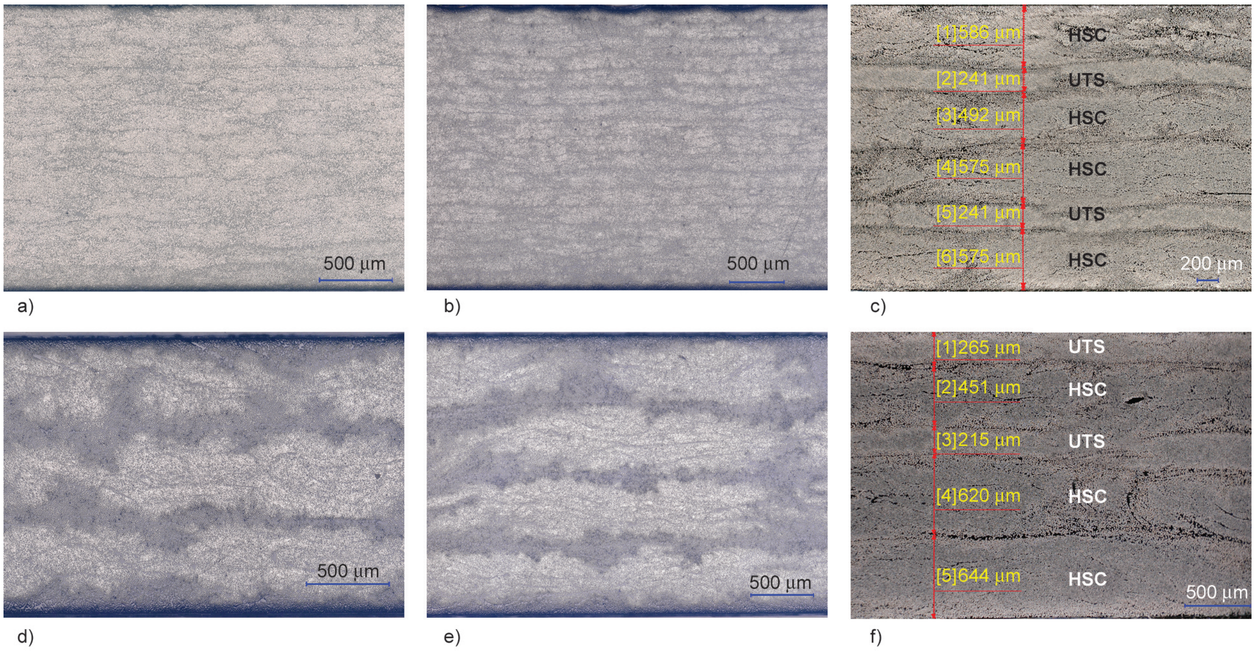

Figure 1. Cross-section views of the materials in this study obtained using a Keyence VHX-5000 series digital microscope; a) UTS13; b) UTS17; c) H2; d) HSC3; e) HSC4; f) H1 [12].

the other unloading stress values, increments of 10 and 15 MPa were considered.

Because the tests were performed in two experimental campaigns, there are small differences in the chosen stress levels for each cycle for the H1 material and the others because H1 tests were performed first, and the stress levels chosen for this material were too high for some of the reference materials. In an additional experimental campaign, the stress levels were kept the same for all tested materials except for the 30° off-axis angles test on UTS13. Initially, higher values were designated for the maximum stress in the cycle. Given that none of the UTS13 samples completed the 6th cycle, adjustments were made to reduce the maximum stress levels in the final cycles for the other materials. The actual values of the unloading stress levels that were imposed for each configuration are detailed in Table 2.

All mechanical tests were carried out at ambient temperature (20 °C) using an electromechanical testing machine INSTRON® 5960 (Instron, Norwood, Massachusetts, USA) with a load cell of 50 kN and controlled in displacement at 1 mm/min, giving an approximate strain rate of 10^{-4} 1/s. As in previous works [12, 29], Digital image correlation (DIC) was used for strain measurements because it is a powerful optical technique that enables non-contact, full-field measurements [30–32]. GOM Aramis® 5M package (GOM Metrology, Braunschweig, Germany) was used for DIC measurements, post-processing, and extraction of the strain values. The GOM Aramis® 5M sensor comprises two charge-coupled device (CCD) cameras with a resolution of 2448×2050 pixels. Lenses with a 50 mm focal distance and no zoom capability were employed. The tensile force from the tensile machine was imported via the Analog-to-digital

Table 2. Maximum stress for each cycle of load-unload tests.

Material	θ	C1 σ_{max} [MPa]	C2 σ_{max} [MPa]	C3 σ_{max} [MPa]	C4 σ_{max} [MPa]	C5 σ_{max} [MPa]	C6 σ_{max} [MPa]
H1	15°	72	145	160	175	190	205
	30°	30	60	70	80	90	100
	45°	22	44	55	65	–	–
H2, HSC3, HSC4, UTS13, UTS17	15°	65	120	140	160	180	190
	45°	20	40	50	60	–	–
H2, HSC3, HSC4, UTS17	30°	25	50	60	70	80	90
UTS13	30°	25	50	70	85	95	100

(A/D) input of the sensor controller to establish a more accurate correlation between force and displacement measurements.
The sample dimensions for all off-axis tensile tests were according to EN ISO 527-5 [33], as illustrated by Figure 2, with the corresponding axis systems: x – the load direction, y – transverse to the load direction, 1 – fiber direction, 2 – transverse to the fiber direction, and θ – the off-axis angle. Additional details of the sample configurations for each material are given in Table 3, as well as the number of tested samples. The samples were provided in two batches and were cut using methods available at the specific time. H1 samples were cut at the manufacturer's facility using a milling machine, while all other samples were cut using water-jet cutting at Université de Bretagne Occidentale in Brest, France. Sample edges were visually inspected to ensure no visible asperities that could affect the tests.
For the DIC analysis, a high-contrast stochastic pattern was applied to the specimen under investigation. Prior to the test, a reference image of the undeformed sample was recorded, followed by sequential images of the deformed sample during the tensile test. The ARAMIS V6.3 software from the GOM Aramis® 5M package was used in the postprocessing step to analyze and track the unique surface patterns, providing a progressive measurement of surface deformation. The DIC processing employed a subset size of 19×19 pixels, with a step size of 10 pixels and an overlap area of 9 pixels. According to the system's user manual, under standard conditions, the standard

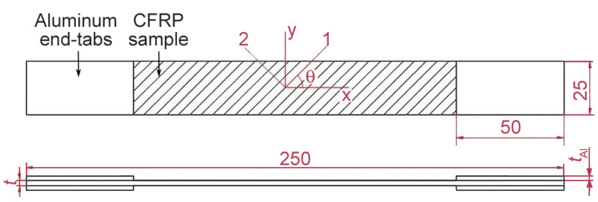

Figure 2. Samples dimensions in mm [12].

deviation for in-plane displacements can reach up to 0.4 µm.
After calibrating the GOM system, only 75 mm of the sample's gauge length was within the field of view of the camera system, out of the total of 150 mm.

4. Residual strain and damage variable estimation

To investigate the cause for nonlinear behavior in off-axis tests for the composite materials, cyclic load-unload tests are performed, with the amplitude of the stress level increasing for each cycle. This approach has been proposed by Ladevèze and LeDantec [28], and they associated the stiffness reduction with a damage variable based on continuum damage mechanics, while a plasticity model takes into account the residual strains with complete unloading.
The damage variable (D) can be calculated from the cyclic load-unload tests using Equation (1), where E_i represents the modulus of the i^th cycle and E_0 represents the initial elastic modulus of the first cycle. The damage variable provides an indirect measurement of physical damage in composite laminates [34]. The residual strain (or plastic strain), needed for identifying the parameters for a plasticity model, can be extracted as well from the cyclic load-unload modulus using Equation (2) where σ_i is the maximum stress in the i^th cycle, which should be as close as possible to the maximum stress levels imposed in the test setup:

$$D = 1 - \frac{E_\mathrm{i}}{E_0} \tag{1}$$

$$\varepsilon_\mathrm{res} = \varepsilon_\mathrm{i} - \frac{\sigma_\mathrm{i}}{E_i} \tag{2}$$

In Ladevèze and LeDantec's work [28], the elastic modulus of the cycle E_i is evaluated as the unloading chord modulus from the endpoints of the loading and unloading part of the ith cycle, as shown in Figure 3a

Table 3. Tensile tests - samples' dimension details, according to EN ISO 527-5 [33] standard.

Laminate	Off-axis angle	Number of samples	Nominal length [mm]	Nominal width, *w* [mm]	Nominal thickness, *t* [mm]	Aluminum tabs thickness, t_{Al} [mm]
HSC3	15°, 30°,45°	3	250	25	1.69	1.5
HSC4	15°, 30°,45°	3	250	25	2.24	1.5
UTS13	15°, 30°,45°	3	250	25	2.10	1.5
UTS17	15°, 30°,45°	3	250	25	2.70	1.5
H1	15°, 30°,45°	4	250	25	2.19	2.0
H2	15°, 30°,45°	1/2/1*	250	25	2.70	1.5

*a limited number of H2 samples were available for each off-axis angle

(Ladevèze method), such that the effects of the load-unload hysteresis are minimized [27]. The same suggestion is given by Lemaitre and Chaboche [35]. Ladevèze's approach to elastic modulus evaluation was also used by Zhai *et al.* [36] to determine damage parameters for a coupled damage-plasticity model for nonlinear off-axis behavior prediction of quasi-UD E-glass fabric reinforced polypropylene composites. In other works [37–39], the same approach was used to evaluate the in-plane shear modulus degradation. Fuller and Wisnom [40] used a similar approach to show that the $[\pm 26_5]_s$ and $[\pm 27_5]_s$ layups of thin-ply carbon-fiber specimens retain most of their initial stiffness after multiple cyclic load-unload testing while exhibiting pseudo-ductility. However, they considered that by calculating the chord modulus of each cycle from a higher applied stress than the previous one, an overestimation of the stiffness loss would be induced and used a secant modulus up to a constant value of applied stress.

While Ladevèze's approach is widely used in the literature, two other proposals for the evaluation of the elastic modulus of the cycle were found, which are less researched. Fitoussi *et al.* [41] suggested taking the cycle modulus as the slope of a linear regression of the reloading curve of the cycle, taken between $\sigma_{xi}/10$ and $\sigma_{xi}/2$. An illustration of this method is found in Figure 3b and is referred to as the Fitoussi method. Castres [43] suggested another approach, by applying a successive linear regression on the loading curve of each cycle and selecting the modulus as the slope of the linear regression that has a maximum coefficient of determination R^2. Castres's proposal is very similar to the method described in previous work [12], and used for the extraction of the apparent modulus from the off-axis tensile test, denoted as the regression method. By considering the tangential modulus of the loading curve, the stress level of the cycle should not influence the modulus evaluation. Compared to the chord modulus, which provides an overall measure of how the material's stiffness changes as it undergoes loading and unloading, capturing the cumulative effect of these changes throughout the cycle, the tangential modulus offers a localized measure of the material's stiffness during the initial loading phase of the cycle. However, it does not account for the energy dissipation and the differences between loading and unloading behavior.

In the regression method employed in this work, for each loading curve of each cycle, successive least-squares linear regressions are employed. For a given cycle, a regression is calculated using an initial selection of the first few experimental points from the entire loading curve. Subsequent regressions are computed by adding additional experimental points with each increment. For each regression, the coefficient of determination R^2 is determined, indicating the correlation between experimental data and the

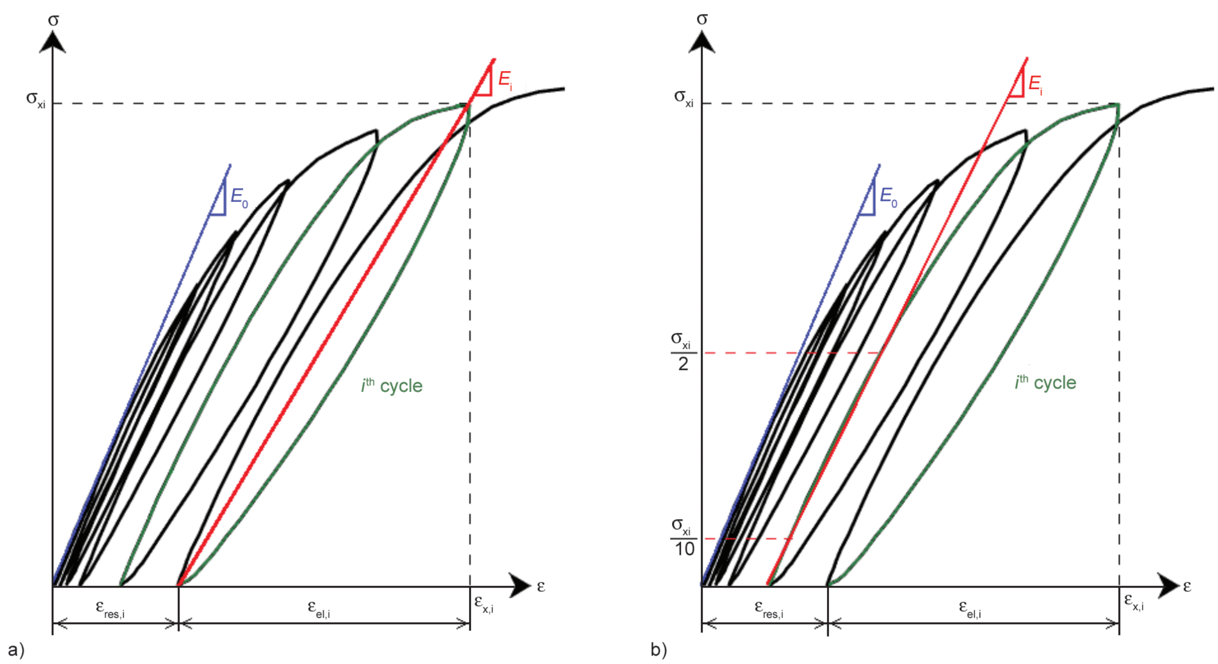

Figure 3. Method of determination of damage variable D and residual strain ε_{res} from load-unload cycles; a) Ladevèze's method (adapted from [28]), b) Fitoussi's method (adapted from [41, 42]).

linear fit. A value of 1 indicates a perfect fit. In this procedure, the dataset points from the loading curve with the highest R^2 are identified, and the apparent modulus is then determined as the slope of the linear fit for the data points associated with the highest R^2 regression.

The distinction between the Fitoussi method and the regression method lies in the data points from the loading curve used to assess the modulus. The Fitoussi method employs linear regression within predetermined bounds on the loading curve, regardless of the fit's quality. In contrast, the regression method selects the set data points from the same loading curve that offers the best correlation to a linear regression. While Eliopoulos and Philippidis [44] also determined the cycle elastic modulus for stiffness degradation analysis as the slope of the linear regression model of each stress–strain loop, no mention is made in their work as to whether any bounds or additional criteria were imposed for the regression.

Regardless of the method for extracting the cycle modulus, in these methods, the residual strain is extracted in the same manner as in Ladevèze's work. The three methods for evaluating the elastic modulus of the cycle, thus the damage variable, are employed and compared in this work and will be referred to as the Ladevèze method, the Fitoussi method, and the regression method.

5. Results and discussion

In general, good reproducibility was obtained for all configurations, thus, only representative samples are presented. Figure 4 shows the axial stress-strain response for representative samples of monotonic and cyclic load-unload, where columns represent the off-axis angle and the rows the laminate configuration. It can be observed that the cyclic envelope curve is coincident with the monotonic curve for all materials at all tested off-axis angles. Only for the 15° off-axis angle, for UTS17, H1, and H2, the cyclic curve shows a small extent of strain hardening as the nonlinear deformation increases.

All cyclic load-unload tensile curves exhibit a nonlinear appearance, with residual strains with complete unloading. It suggests that the cause of the nonlinearity of the stress-strain response involves a plastic component. Moreover, the nonlinearity of the stress-strain curves during unloading was also observed, which leads to a decreased elastic modulus that has been attributed to internal damage [28, 36, 45].

Similar to monotonic off-axis results from a previous study [12], UTS laminates exhibit a visible, more pronounced nonlinearity with increasing load compared to HSC and hybrid laminates. Furthermore, for UTS13, the residual strain appears to be significantly higher than for other laminates for the 15° and 30° off-axis angles. Moreover, all cyclic load-unload tensile curves exhibit hysteresis loops, with the width of the hysteresis loop decreasing with increasing off-axis angle. A similar observation was made by Kawai and Negishi [46] for AS4/PEEK unidirectional composites. While studying the ratcheting behavior of unidirectional T300/7901carbon fiber composites loaded off-axis, Cheng *et al.* [47] observed that the nonlinear hysteresis behavior and ratcheting effect of each specimen under asymmetric stress cycles depend on the fiber orientation and peak loading stress. The size and shape of the hysteresis loop in each cycle remained unchanged for 100 cycles. Thus, it can be implied that the wider hysteresis loops with increasing cycle number, as well as decreasing off-axis angles, are due to the increase in the maximum stress levels imposed for the cycles.

5.1. Residual strain estimation

The first to be investigated is the residual strain. Figure 5 illustrates the average residual strain at the unloading point versus the total strain of the cycle. Throughout this work, all error bars represent half the measuring range for samples tested in the same configuration.

For all configurations, the residual strain rapidly accumulates with each cycle, and its value increases as the prior maximum stress becomes larger, as also noted by Kawai and Negishi [46]. It also shows a dependence on the fiber orientation, as the residual strain in 15° samples is the highest and in 45° samples is the lowest. This could be due to the fact that for 15° off-axis tests, higher stress values for each cycle are imposed, compared to other off-axis angles. Moreover, for 15° samples, the residual strain has a sharp increase towards the last three cycles, while for 45° samples, the increase is almost linear after the second cycle. Again, the higher values imposed for 15° samples could be responsible. Moreover, a lower number of cycles was imposed for the 45°off-axis angle (4 cycles are imposed as opposed to 6 for the other angles). For all cases, the maximum stress for the first two cycles is chosen to be in the linear response regime, and as close to the transition

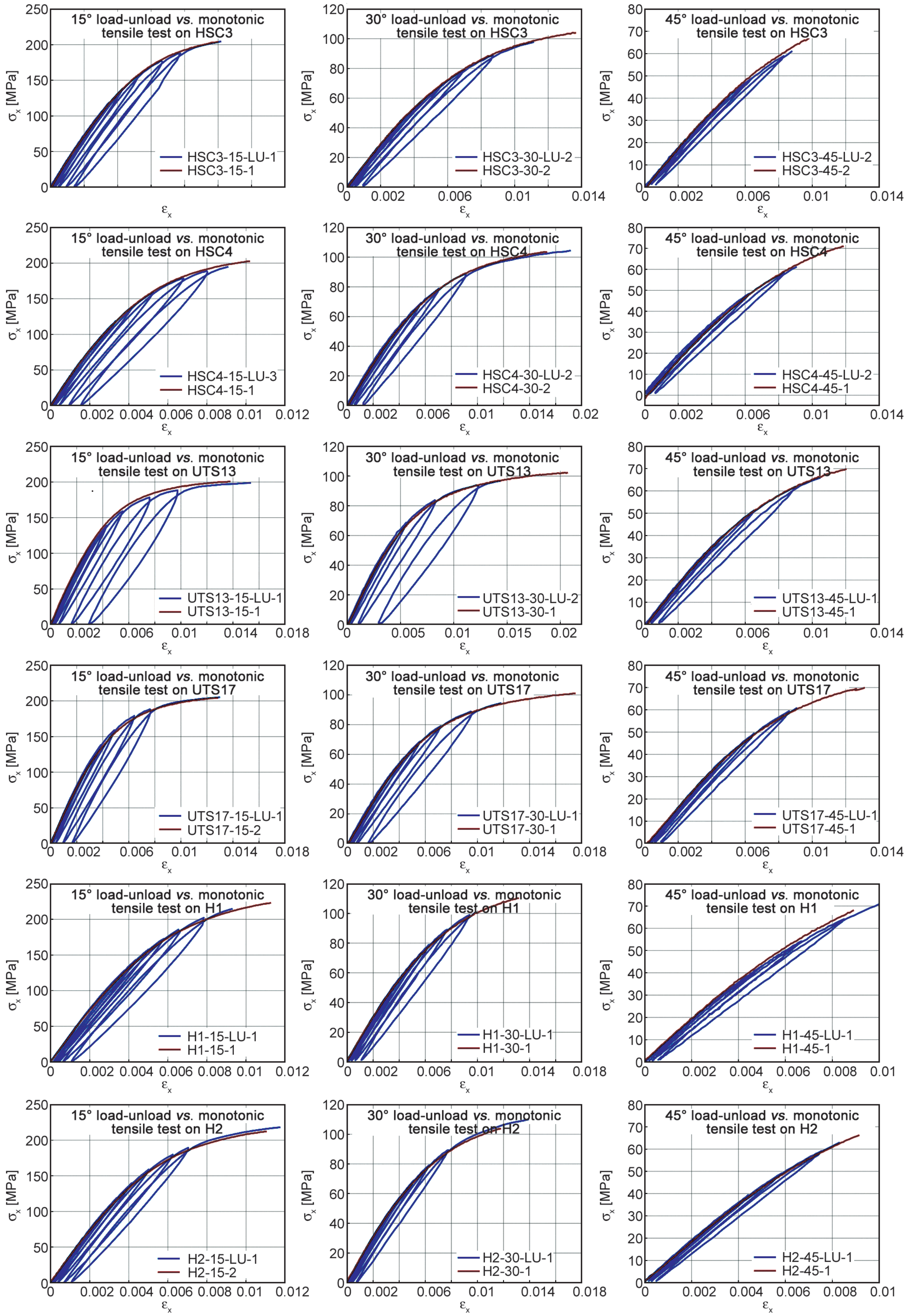

Figure 4. Axial stress-strain response of representative samples for monotonic and load-unload off-axis tensile tests with columns representing off-axis angles and the rows the laminate configuration.

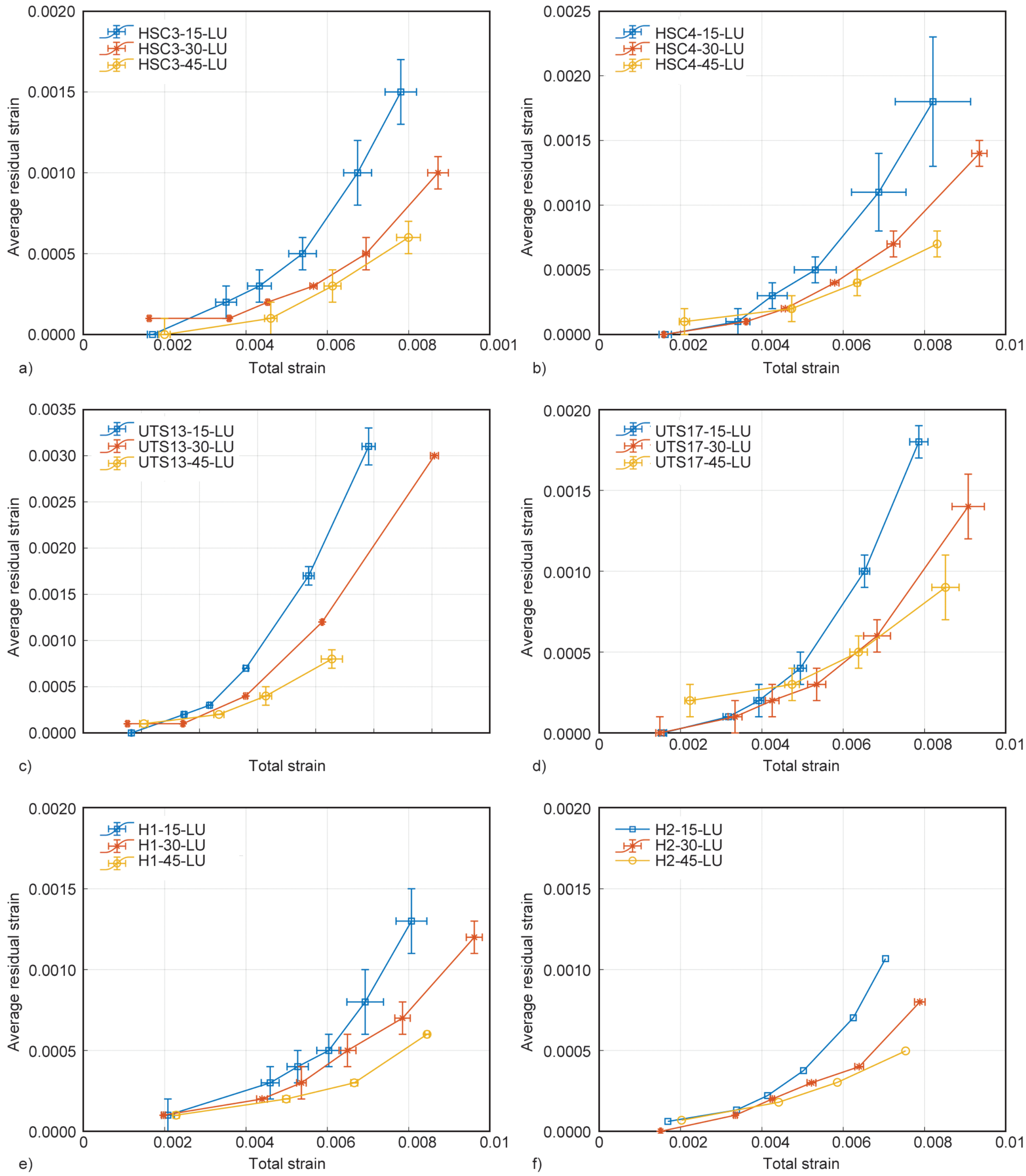

Figure 5. Average residual strain *vs*. average total strain; a) HSC3; b) HSC4; c) UTS13; d) UTS17; e) H1; f) H2.

point from linear to nonlinear response, leading to similar residual strain accumulation, regardless of the off-axis angle.

Furthermore, it was shown by Sinclair and Chamis [48] that when loaded off-axis, the fracture surfaces of unidirectional composites revealed resulted in distinct fracture modes based on the off-axis angles. Up to 30°, the fracture is mainly due to intralaminar shear stress, whereas fracture at 45° primarily indicates failure due to transverse tensile stress. Consequently, the different failure mechanisms could contribute to the observed differences in residual strain accumulation at different off-axis angles.

Figures 6a, 6b, and 6c show a comparison of average residual strain versus average total strain between all tested materials, and in Figures 6d, 6e, and 6f, a comparison of moderate residual strain vs. cycle stress level is presented. By looking at the results from cyclic load-unload tests for 15° and 30° off-axis angles (1st column – 15°; 2nd column – 30°), it can be

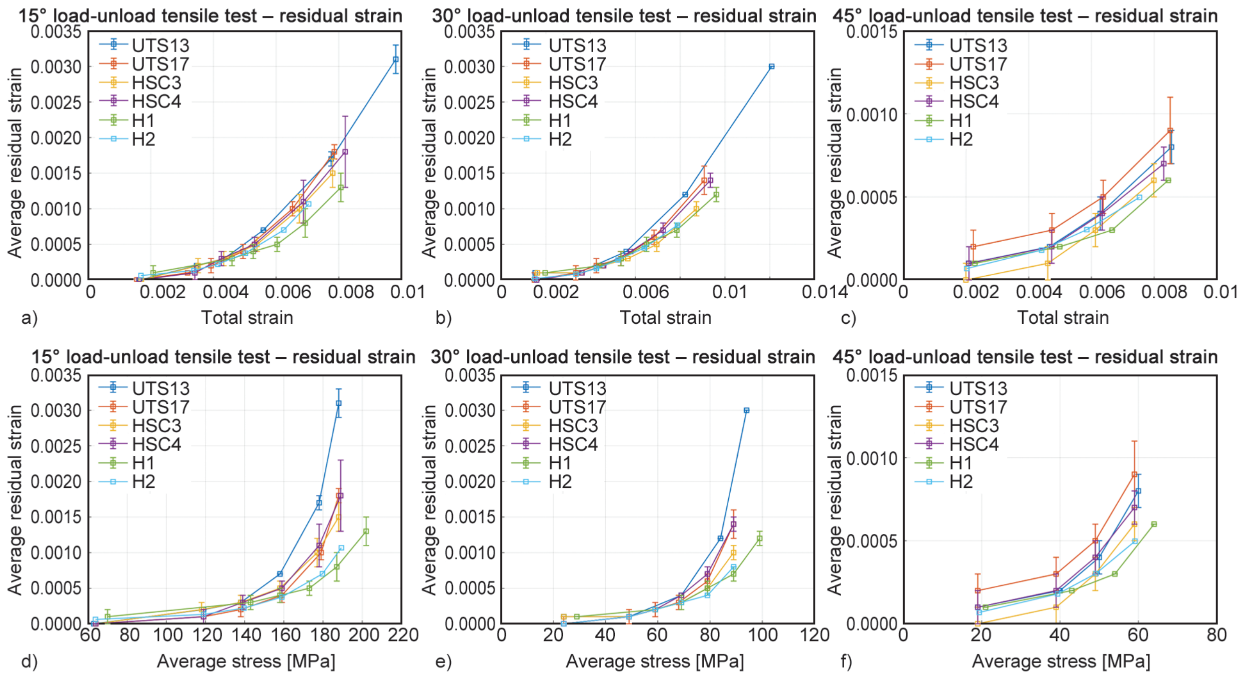

Figure 6. Comparison of average residual strain *vs*. cycle stress level: a) 15°; b) 30°; c) 45°; Comparison of average residual strain *vs*. total strain: d) 15°; e) 30°; f) 45°.

observed that in both cases, UTS13 has the highest residual strain, and it also reaches a significantly higher total strain by the last cycle, compared to other materials. Still, when analyzing the average residual strain versus average total strain (Figure 6a and Figure 6b), the evolution trend of the residual strain of UTS13 is similar to the evolution trend for UTS17, it only reaches higher values of both residual strain and total strain.

If the evolution trend of average residual strain versus average maximum stress of the cycle (the value imposed in the test setup) is analyzed for the same stress levels, the residual strain of UTS13 has a sharper increase than UTS17, with a residual strain value of 1.7 times higher for the last cycle of 15° off-axis load-unload test. For the 45° off-axis angle (Figure 6c and Figure 6f), the shape of the residual strain evolution is similar for UTS13 and UTS17, with UTS17 having higher values. Overall, UTS laminates have the highest residual strains in all test cases, suggesting that the matrix in UTS prepreg has an inherent higher plasticity characteristic compared to HSC laminates.

The residual strains of HSC3 and HSC4 laminates have similar evolution for each off-axis angle, with very close values for the 15° off-axis angle. For the 30° and 45° off-axis angles, HSC4 has a higher increase in residual strain towards the last cycles compared to HSC3. A similar trend is also observed for the hybrid laminates, H1 and H2. In this case, the close values of residual strain are found for the 30° off-axis angle, while for 15° and 45° off-axis angles, H2 shows an increased residual strain towards the last cycles. Furthermore, it can be observed that in all cases, the hybrid laminates have lower residual strains compared to all reference laminates for similar total strains. This fact suggests that the interaction between the different prepreg plies within the hybrid carbon laminates leads to a material with fewer residual strains, thus a more stable material with a better ability to recover from displacements [49]. The lower residual strain for hybrid laminates, compared to HSC laminates could also be attributed to the fact that the hybrid laminates have less resin-rich regions compared to HSC laminates.

While there is a difference in the amount of accumulated residual strain for laminates of the same prepreg type with different thicknesses, for UTS laminates, the thinner laminate exhibits a higher residual strain than the thicker laminate, and for HSC laminates the opposite occurs – the thicker laminate has a higher residual strain compared to the thinner one, for 15° and 30° off-axis angles, whereas for 45° off-axis angle, the thicker composite exhibits a higher residual strain than the thinner laminate, for both UTS and HSC composites. Although a thickness effect on the residual strain with complete unloading might exist, no clear conclusion can be drawn for the tested laminates, and additional testing at different angles and thicknesses would be required to observe a relevant trend.

5.2. Damage variable evaluation

For the estimation of the damage variable, the three methods mentioned in Section 4 were used. Examples of the results following the application of the three methods for the same individual sample are given in Figure 7. For all three examples, it is observed that Ladevèze's method gives overall higher damage variable values, with an almost linear increase with applied stress level. The damage variables calculated based on the Fitoussi and regression model have lower values, closer to each other for the first cycles. This outcome was expected, as Ladevèze's method considers the unloading chord modulus of the cycle, which is lower in value than the modulus given by the loading curve of the cycle, considered in the other two methods.

It is also observed that for some cycles, the damage variable evaluated with Fitoussi's method or the regression method presents negative values. While the damage parameter accounts for stiffness loss due to internal damage, we consider that the negative values do not retain any physical meaning, as damage growth is an irreversible phenomenon [35, 50]. Therefore, the negative values of the damage variable represent a procedural error of the employed methods for evaluating the cycle modulus. Due to the cycle hysteresis loop, as well as to noise in the data for the first two cycles, the modulus extracted with Fitoussi's method and the regression model has a close value or even higher than the modulus extracted from the 1st cycle in some cases. This leads to negative values of the damage variable or lower values compared to previous cycles when employing Equation (1). Thus, the damage variable growth with increasing stress does not have a smooth evolution for the Fitoussi and regression model, as it has for the Ladevèze method, with the regression model having the most irregular progression. Although Eliopoulos and Philippidis [44] also employed a linear regression for each stress–strain loop to extract

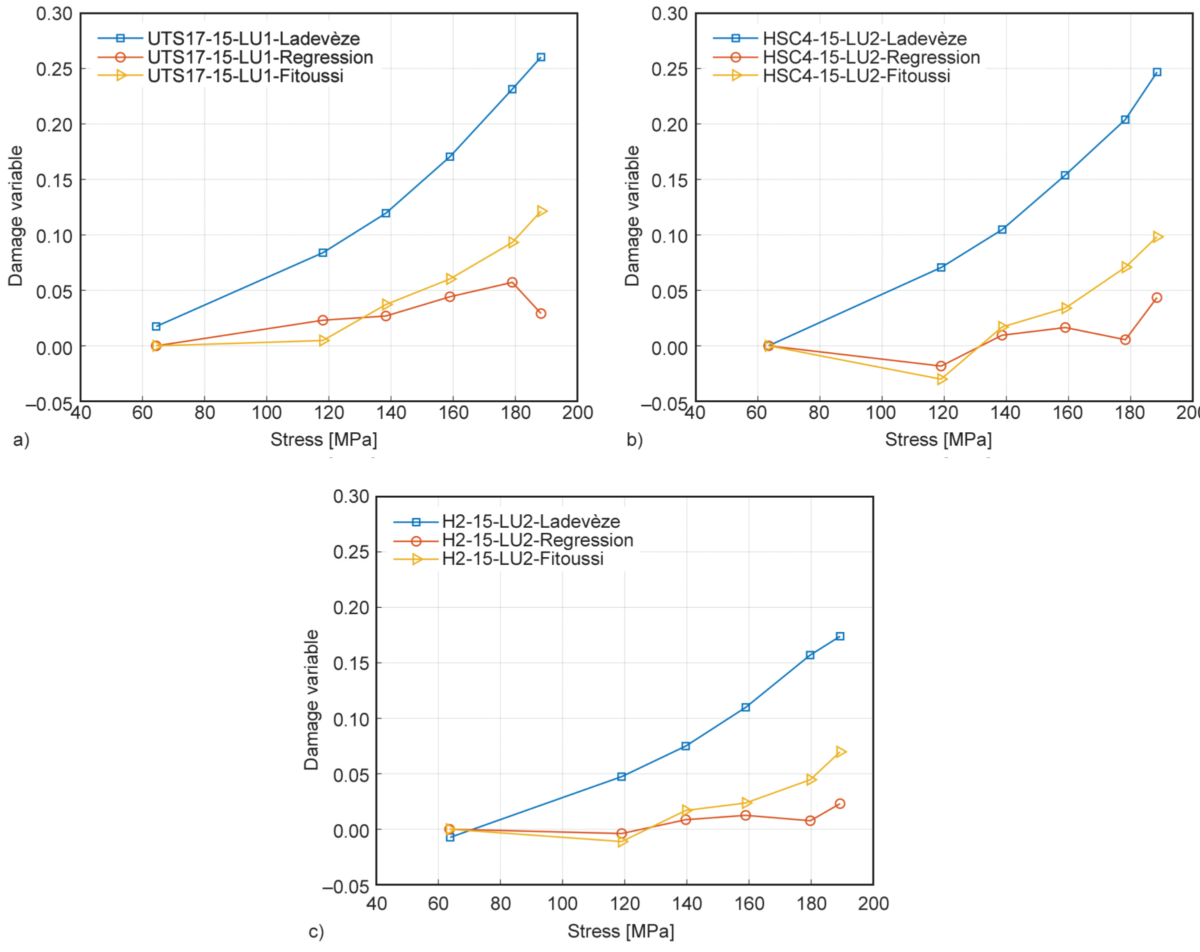

Figure 7. Application of Ladeveze, regression, and Fitoussi methods to evaluate the damage variable from 15° off-axis cyclic load-unload tensile test; a) UTS17 – sample 1; b) HSC4 – sample 2; c) H2 – sample 1.

the cycle modulus of $[\pm 45]_s$ GFRP composites, they did not report a higher modulus evaluation for subsequent cycles.

Figure 8 shows the average damage variable estimated using all three methods, for all off-axis angle/material configurations, with error bars as half of the measuring range. It can be observed that for all off-axis angles, the Ladevèze method gives the highest value for the damage variable, with a smooth increase with increasing applied stress. Based on the Fitoussi and regression methods, the average damage variables have lower values compared to the Ladevèze method, and they are closer together in the first cycles, as previously mentioned, for the analysis of the results on an individual sample.

The evolution of the damage variable estimated using the regression and Fitoussi methods is smoother at 45° off-axis angle, pointing to a potential influence of the hysteresis loop width on the cycle elastic modulus extraction.

There are high error bars in all results of all three methods. This suggests that despite similar cycle-load-unload stress-strain responses between samples of the same configuration, there is a difference in stiffness reduction with increasing applied stress. Even though samples are of the same configuration, they might still exhibit slight variations in terms of material properties, imperfections, defects such as voids, or local variations in microstructure. These localized internal differences between samples could lead to early fiber/matrix interface debonding and matrix microcracks, which could lead to a loss in stiffness. A higher error bar is reported in the regression method as compared with the other two, and the damage variable changes at an irregular rate when stress levels increase.

Given that both the Fitoussi method and the regression method share the same fundamental approach to estimating the initial modulus, albeit with distinct data bounds for linear regression, it becomes evident that as the cycles progress, especially in the later cycles where the hysteresis loop widens, and lower off-axis angles (see Figure 4), the selection of data points for cycle modulus estimation becomes a critical factor. Figure 9 shows an example of elastic modulus extraction from the reloading curve of the 5^{th} cycle of a UTS13 sample tested at a 15° off-axis angle, providing both the coefficient of correlation R^2 and the resultant modulus from the linear fit using the selected data. Applying Fitoussi's method with specified data bounds (Figure 9b) yields a strong correlation with $R^2 = 0.9995$ and an apparent modulus $E_x = 34.78$ GPa.

Meanwhile, implementing the regression method on the same reloading curve (Figure 9c) also yields a correlation coefficient of $R^2 = 0.9995$, but with a different data selection closer to the start of the reloading curve, resulting in a higher apparent modulus $E_x = 35.54$ GPa.

Given the initial modulus for this sample ($E_0 =$ 37.70 GPa) Equation (1) calculates a damage variable of 0.07 with Fitoussi's method and 0.05 with the regression method.

Moving on to the 6^{th} cycle of the same sample, Fitoussi's method yields an apparent modulus of 33.05 GPa with $R^2 = 0.9992$, while the regression method provides an apparent modulus of 35.24 GPa with $R^2 = 0.9998$, thus an even greater difference. Although the correlation coefficients remain highly favorable for both methods, the distinction in the data points selected for extraction, specifically the inclusion of experimental points closer to the start of the reloading curve, significantly impacts the modulus value and, subsequently the damage variable value. When comparing the modulus extracted using the Fitoussi and the regression models for all tested samples, percentage differences up to 24% are observed between the values obtained from both approaches.

Thus, one contributing factor to potentially inconsistent results with the regression method is the lower limit imposed for initiating the analysis. In this specific case, an inferior strain limit of 10^{-4} above the first strain value of the reloading curve was established to exclude just the initial few points of the reloading curve, aiming to prevent additional errors induced by potential instability at the start of the reloading curve. This approach avoids introducing instability-associated errors, as no recovery time is mandated in the cyclic test following unloading.

When applying the same lower strain limits to the regression method as used in Fitoussi's method, the same results are obtained for the 5^{th} cycle with both methods. However, for the 6^{th} cycle, the regression method chooses a distinct and shorter dataset, resulting in a stronger correlation and a higher cycle modulus compared to the Fitoussi method.

While effective in extracting the apparent elastic modulus in the case of nonlinear stress-strain curves from off-axis tensile testing [12], the influence of the

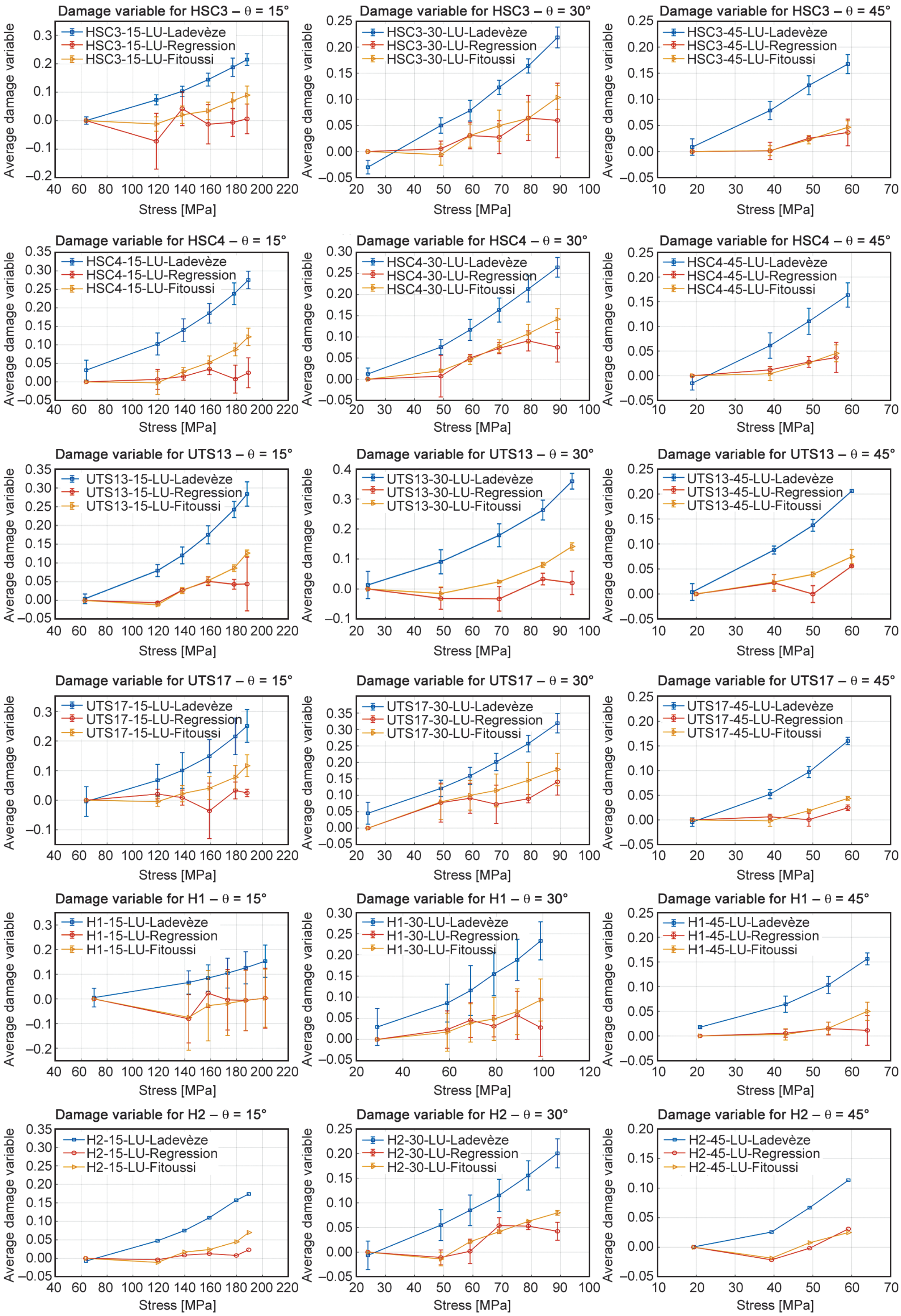

Figure 8. Average damage variables estimated using Ladeveze, Fitoussi, and regression methods with columns representing off-axis angles and the rows the laminate configuration.

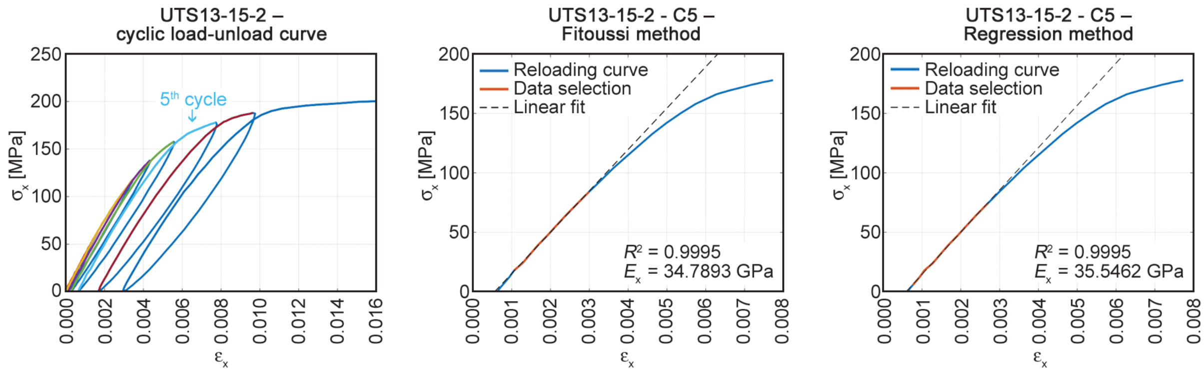

Figure 9. Example of elastic modulus evaluation from the reloading curve; a) cyclic load-unload stress-strain curve for UTS13 sample, 15° off-axis angle; b) elastic modulus evaluation from the reloading curve of the 5th cycle with the Fitoussi method; c) elastic modulus evaluation from the reloading curve of the 5th cycle with the regression method.

chosen inferior limit for employing the regression method on the results highlights a need for a standardized method to evaluate the cycle apparent modulus for composite materials, for low cycle numbers (not fatigue analysis) and increasing cycle amplitude tests.
In Figure 10, a comparison of the average damage variables evolution with total strain, obtained from different off-axis angles, is presented. The total strain was chosen for the x-axis of this plot because of the different stress levels imposed for the cycles for the different off-axis angles. The damage variables estimated using Ladevèze's method are shown in the first column, in the second column the damage variables estimated using Fitoussi's method are shown, and in the third column, the damage variables calculated using the regression model are illustrated.
For all materials, it can be observed that the regression method offers inconclusive results, with an erratic variation of the damage variable with the total strain. By analyzing the evolution with the total strain of the damage variable estimated using Ladevèze's method, for 15° and 30° off-axis angles, the damage variable evolutions are similar, almost linear, with a difference in value for most materials. For Fitoussi's method, the damage variables for 15° and 30° off-axis angles are almost coincident for HSC3 and HSC4, and for other materials, the variation has a similar shape, with a difference in the estimated values. After the second cycle, the evolution of the damage variable is almost linear. It can also be observed that using Ladevèze's method, for HSC3 and HSC4, the damage variable in the 15° off-axis angle case is the highest, while for UTS13 and UTS17 the highest values are found for the 30° off-axis angle. H1 follows the trend of UTS laminates while H2 shows close results for both angles. By using Fitoussi's method, this observation is valid for UTS17, H1, and H2, while for HSC3, HSC4, and UTS13, the results are reversed.
For the 45° off-axis angle, the values of the damage variable are lower compared to other angles, regardless of the method used for extracting the values, except for H1 for which the lowest values are found for the 15° off-axis angle (by using the regression or Fitoussi's method), but with large error bars, implying that the presence of unaccounted-for microstructural variations and internal defects among samples likely influenced the final results for this specific case. When loaded at a 45° off-axis angle, fiber-matrix interfaces are the most loaded, leading to fiber-matrix interface debonding at lower stresses [51], compared to the other angles. Furthermore, interface debonding primarily affects the composite's ability to carry transverse loads, with a more pronounced negative impact at the 45° off-axis angle than at lower off-axis angles. Consequently, at the 45° angle, damage accumulation is constrained as the ultimate failure of the matrix promptly follows interface debonding. Thus, in the 45° off-axis angle case, the unidirectional composite is capable of sustaining a comparably larger loss in modulus and accumulation of residual strain before final failure. Therefore, the damage variable estimation is influenced by the off-axis angle.
A comparison of the damage variables of all material types at the same off-axis angle, using all three methods, is given in Figure 11, with columns representing off-axis angles and the rows the method employed. Again, due to the unpredictable evolution of the damage variable extracted using the regression method, the results are inconclusive, with negative values for some materials and high error bars.

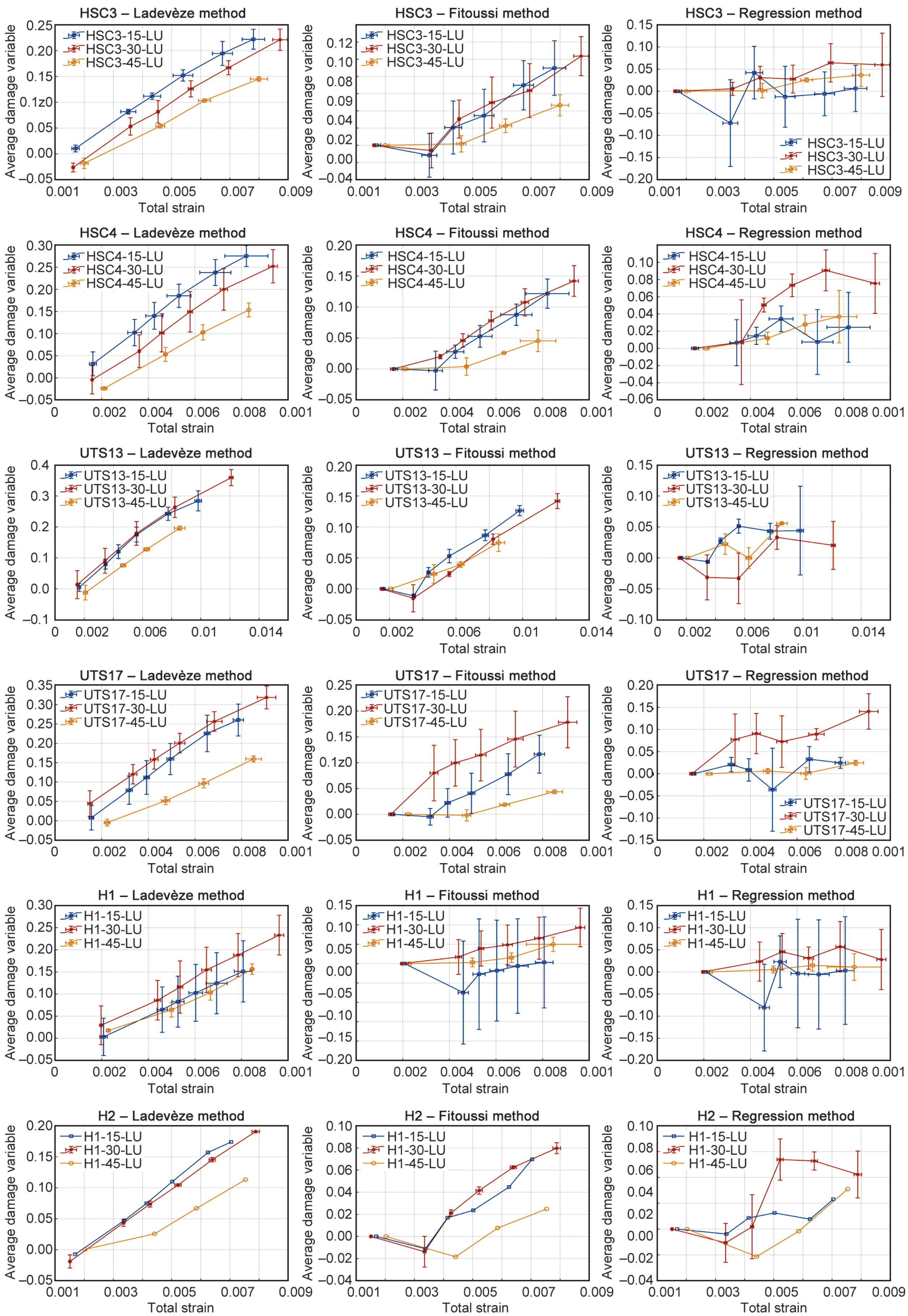

Figure 10. Comparison of average damage variables estimated using Ladeveze, Fitoussi, and regression methods at different off-axis angles with columns representing the method employed and the rows the laminate configuration.

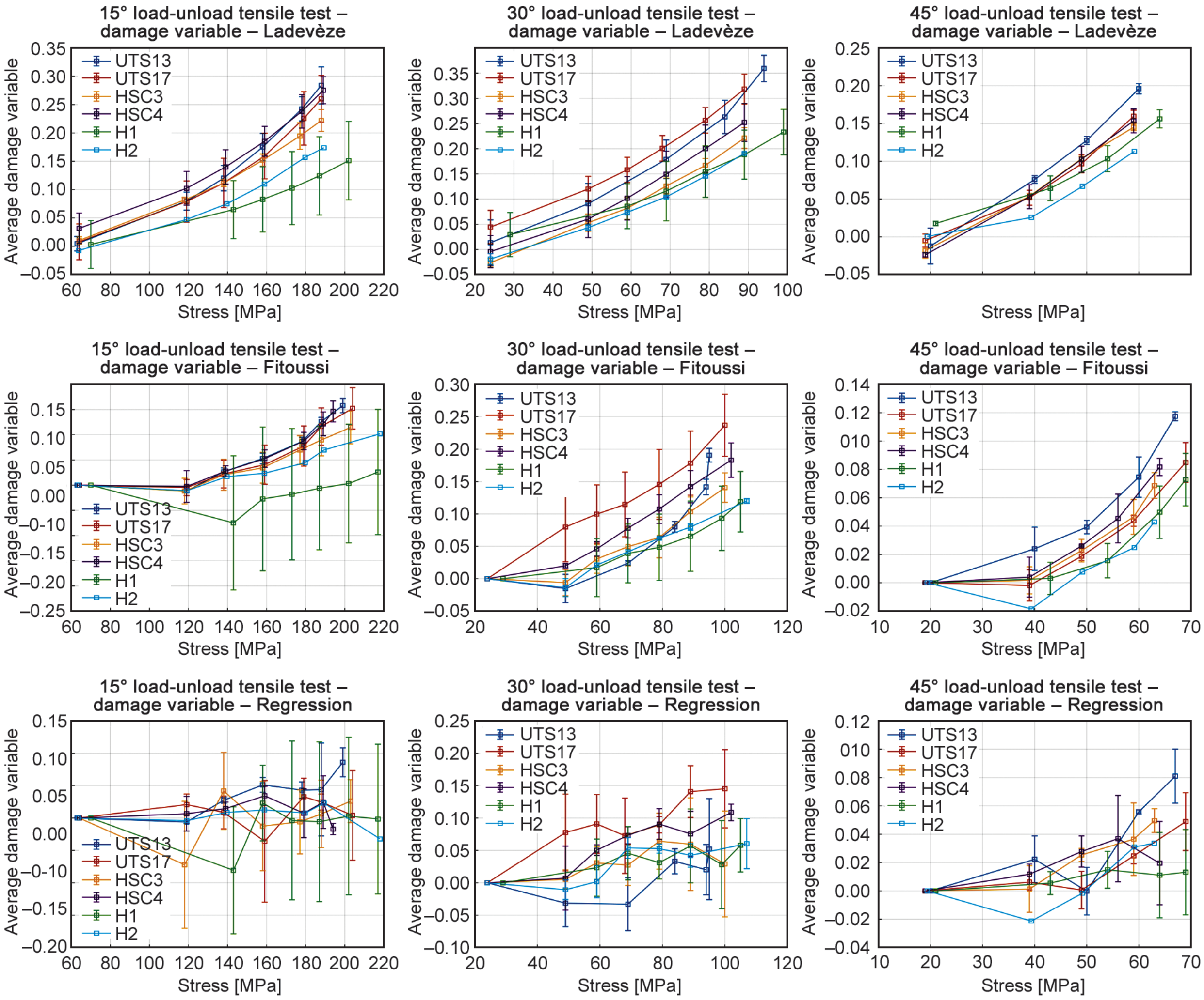

Figure 11. Comparison of the average damage variables estimated using Ladeveze, Fitoussi, and regression methods for the different laminates at the same off-axis angle, with columns representing off-axis angles and the rows the method employed.

For the other two methods, it is clear that the hybrid laminates, H1 and H2, have the lowest damage variables for all off-axis angles. The damage variable increases with increasing maximum stress of the cycle and is closer to a linear evolution for the hybrid laminates, as opposed to the reference laminates for which the damage variable has a sharper increase towards the last cycles. Moreover, it can be observed that for the 15° off-axis angle, the HSC3 and UTS laminates have similar damage variables, and starting with a stress level of 140 MPa, the damage variables of UTS13 and UTS17 diverge from the original path, having higher values than HSC3. For 30° off-axis angles, the damage variable evolutions are almost parallel to each other, with UTS laminates having the highest values. In the case of 45° off-axis angles, the reference laminates present a linear variation of the damage variable with a higher slope compared to hybrid laminates.

By coupling these observations with the ones for the evolution of the residual stress, illustrated in Figure 6, an explanation can be drawn for the off-axis response comparison from a previous study [12], where hybrid laminates exhibited a higher stress level at the same strain compared to reference laminates, in the non-linear response region. UTS laminates exhibit both the highest residual strain and damage variable, thus, with increasing stress levels, the nonlinear response is more pronounced due to internal damage and plasticity of the matrix. HSC laminates do not have such a strong nonlinear off-axis response as UTS laminates, and their residual strains and damage variables are also lower compared to UTS laminates. By combining these two types of plies into H1 and

H2 hybrid configurations, lower residual strains and damage variables are obtained for all off-axis angles, compared to UTS and HSC laminates. Therefore, with less internal damage and plasticity of the matrix, the hybrid configurations show a strain hardening in the off-axis response, reaching a higher stress level at the same strain for all off-axis angles, compared to reference laminates. Thus, a positive hybrid effect is obtained.

5. Conclusions

In this study, we employed the ply-level hybridization technique to achieve a combination of different ply thicknesses and material quality within the same laminate. Cyclic load-unload off-axis testing was performed to investigate the cause of the nonlinear response of the studied laminates, and was concluded that the nonlinearity is caused by a combination of internal damage and residual strain. The evolution of the damage variable and the accumulated residual strain were quantified by analyzing the incremental loading/unloading stress-strain response of the tested samples.

Overall, UTS laminates have the highest residual strains in all test cases, suggesting that the matrix in UTS prepreg has an inherent higher plasticity characteristic compared to HSC laminates, while the hybrid laminates have the smallest residual strains of all materials. The residual strain rapidly accumulates with increasing cycle number and cycle stress level for 15° and 30° off-axis angle, while for 45° off-axis angle, an almost linear evolution of the residual strain with total strain was noticed, suggesting an influence of the off-axis angle on the residual strain. Although a thickness effect on the residual strain with complete unloading might exist, no clear conclusion can be drawn for the tested laminates, and additional testing at different angles and thicknesses would be required to observe a relevant trend.

Three methods were employed to extract the cycle modulus to determine the damage variable: Ladevèze, Fitoussi, and regression. Ladevèze's method gives a higher damage variable, but when selecting the chord modulus for stiffness loss evaluation, there's a potential for overestimating the loss. Among the three methods, the regression method was found to yield inconclusive results, as the damage variable changes at an irregular rate when stress levels increase, giving also negative values and large error bars. However, it was noticed that the selection of the starting data point for the application of the regression method influences the results. Moreover, the data points for estimating the elastic modulus from the loading curve can yield discrepancies in the values of the modulus. When comparing results using the Fitoussi method and the regression method for the same loading curves, percentage differences of up to 24% in modulus values were identified between these methods. Therefore, there's a requirement to establish a standardized strain threshold that avoids potential errors introduced during the initial phase of the reloading curve, all while accounting for potential strain hardening/softening due to load-unload cycles. Such standardization could lead to reliable results from the regression method.

An influence of the off-axis angle on the damage accumulation was noticed as well, and it was attributed to the different fracture modes between 15°–30 °off-axis samples and 45° off-axis samples.

In terms of hybridization effects, it was noticed that the hybrid configurations exhibit lower residual strains and damage variables for all off-axis angles, compared to reference UTS and HSC laminates, leading to a positive hybrid effect. With less internal damage and plasticity of the matrix, the hybrid configurations show a strain hardening in the off-axis response compared to reference ones, being able to reach higher stress levels at the same strain.

The findings of this study also lay the groundwork for defining damage and plasticity parameters essential for predictive tools concerning the off-axis nonlinear behavior of fiber-reinforced composite materials. By integrating the damage variable results obtained through these methods into such a predictive tool, a feasible approach emerges for comparing outcomes and assessing which method offers a more precise representation of nonlinear behavior evolution and, consequently more accurate damage parameters. This objective stands at the forefront of future research efforts.

Acknowledgements

The first author acknowledges the financial support of Campus France for internships at ENSTA Bretagne, where the experimental tests were conducted. The authors also express gratitude to Belcoavia S.R.L. for manufacturing the composite plates, Thomas Bonnemains from IUT Brest for water-jet cutting of the samples, and the staff at ENSTA Bretagne, particularly Claudiu Bădulescu, for their guidance and assistance with the experimental equipment.

References

[1] Pawlak A. M., Górny T., Dopierała Ł., Paczos P.: The use of CFRP for structural reinforcement – Literature review. Metals, **12**, 1470 (2022). https://doi.org/10.3390/MET12091470

[2] Curtis P. T., Browne M.: Cost-effective high performance composites. Composites, **25**, 273–280 (1994). https://doi.org/10.1016/0010-4361(94)90219-4

[3] Audibert C., Andreani A-S., Lainé É., Grandidier J-C.: Mechanical characterization and damage mechanism of a new flax-Kevlar hybrid/epoxy composite. Composite Structures, **195**, 126–135 (2018). https://doi.org/10.1016/j.compstruct.2018.04.061

[4] Zuo P., Srinivasan D. V., Vassilopoulos A. P.: Review of hybrid composites fatigue. Composite Structures, **274**, 114358 (2021). https://doi.org/10.1016/j.compstruct.2021.114358

[5] Naito K., Yang J-M., Kagawa Y.: Tensile properties of high strength polyacrylonitrile (PAN)-based and high modulus pitch-based hybrid carbon fibers-reinforced epoxy matrix composite. Journal of Materials Science, **47**, 2743–2751 (2012). https://doi.org/10.1007/S10853-011-6101-8

[6] Czél G., Jalalvand M., Wisnom M. R., Czigány T.: Design and characterisation of high performance, pseudo-ductile all-carbon/epoxy unidirectional hybrid composites. Composites Part B: Engineering, **111**, 348–356 (2017). https://doi.org/10.1016/j.compositesb.2016.11.049

[7] Dransfeld C., Amacher R., Cugnoni J., Brunner J., Kramer E., Smith W., Scobbie K., Sorensen L., Botsis J.: Toward aerospace grade thin-ply composites. in 'Proceeding of the 17th European Conference on Composite Materials. Munich, Germany' 1–9 (2016).

[8] Furtado C., Arteiro A., Catalanotti G., Xavier J., Camanho P. P.: Selective ply-level hybridisation for improved notched response of composite laminates. Composite Structures, **145**, 1–14 (2016). https://doi.org/10.1016/j.compstruct.2016.02.050

[9] Sebaey T. A., Mahdi E.: Using thin-plies to improve the damage resistance and tolerance of aeronautical CFRP composites. Composites Part A: Applied Science and Manufacturing, **86**, 31–38 (2016). https://doi.org/10.1016/j.compositesa.2016.03.027

[10] Sasikumar A., Trias D., Costa J., Blanco N., Orr J., Linde P.: Effect of ply thickness and ply level hybridization on the compression after impact strength of thin laminates. Composites Part A: Applied Science and Manufacturing, **121**, 232–243 (2019). https://doi.org/10.1016/j.compositesa.2019.03.022

[11] Amacher R., Cugnoni J., Botsis J., Sorensen L., Smith W., Dransfeld C.: Thin ply composites: Experimental characterization and modeling of size-effects. Composites Science and Technology, **101**, 121–132 (2014). https://doi.org/10.1016/j.compscitech.2014.06.027

[12] Casapu M., Arrigoni M., Fuiorea I.: Off-axis response and shear characterization of unidirectional ply-level hybrid carbon-fiber-reinforced polymer materials. Incas Bulletin, **15**, 31–46 (2023). https://doi.org/10.13111/2066-8201.2023.15.3.3

[13] Hahn H. T., Tsai S. W.: Nonlinear elastic behavior of unidirectional composite laminae. Journal of Composite Materials, **7**, 102–118 (1973). https://doi.org/10.1177/002199837300700108

[14] Ogihara S.: Nonlinear mechanical response of CFRP laminates under off-axis tensile loading. Science and Engineering of Composite Materials, **17**, 133–141 (2010). https://doi.org/10.1515/secm.2010.17.2.133

[15] Yokozeki T., Ogasawara T., Ishikawa T.: Nonlinear behavior and compressive strength of unidirectional and multidirectional carbon fiber composite laminates. Composites Part A: Applied Science and Manufacturing, **37**, 2069–2079 (2006). https://doi.org/10.1016/j.compositesa.2005.12.004

[16] Ma Y., Li Y., Liu L.: Off-axis tension behaviour of unidirectional PEEK/AS4 thermoplastic composites. Applied Sciences, **13**, 3476 (2023). https://doi.org/10.3390/APP13063476

[17] Sun C. T., Chen J. L.: A simple flow rule for characterizing nonlinear behavior of fiber composites. Journal of Composite Materials, **23**, 1009–1020 (1989). https://doi.org/10.1177/002199838902301004

[18] Cho J., Fenner J., Werner B., Daniel I. M.: A constitutive model for fiber-reinforced polymer composites. Journal of Composite Materials, **44**, 3133–3150 (2010). https://doi.org/10.1177/0021998310371547

[19] Batra R. C., Gopinath G., Zheng J. Q.: Material parameters for pressure-dependent yielding of unidirectional fiber-reinforced polymeric composites. Composites Part B: Engineering, **43**, 2594–2604 (2012). https://doi.org/10.1016/j.compositesb.2011.12.005

[20] Vogler M., Koerber H., Kuhn P., Rolfes R., Camanho P.: Constitutive modeling and experimental characterization of the non-linear stress-strain behavior of unidirectional carbon-epoxy under high strain rates. in 'Proceeding of the 20th International Conference on Composite Materials. Copenhagen, Denmark' 1–10 (2015).

[21] Petit P. H., Waddoups M. E.: A method of predicting the nonlinear behavior of laminated composites. Journal of Composite Materials, **3**, 2–19 (2016). https://doi.org/10.1177/002199836900300101

[22] Matzenmiller A., Lubliner J., Taylor R. L.: A constitutive model for anisotropic damage in fiber-composites. Mechanics of Materials, **20**, 125–152 (1995). https://doi.org/10.1016/0167-6636(94)00053-0

[23] Chen Y., Zhao Y., Ai S., He C., Tao Y., Yang Y., Fang D.: A constitutive model for elastoplastic-damage coupling effect of unidirectional fiber-reinforced polymer matrix composites. Composites Part A: Applied Science and Manufacturing, **130**, 105736 (2020). https://doi.org/10.1016/j.compositesa.2019.105736

[24] Vasiukov D., Panier S., Hachemi A.: Non-linear material modeling of fiber-reinforced polymers based on coupled viscoelasticity–viscoplasticity with anisotropic continuous damage mechanics. Composite Structures, **132**, 527–535 (2015).
https://doi.org/10.1016/j.compstruct.2015.05.027

[25] Wang Y., Chen D., Li N., Yuan H., Zhu Z., Li Y., Huang Z.: A micromechanics based elasto-plastic damage model for unidirectional composites under off-axis tensile loads. Scientific Reports, **10**, 847 (2020).
https://doi.org/10.1038/s41598-020-57771-8

[26] Schuecker C., Pettermann H. E.: Combining elastic brittle damage with plasticity to model the non-linear behavior of fiber reinforced laminates. Computational Methods in Applied Sciences, **10**, 99–117 (2008).
https://doi.org/10.1007/978-1-4020-8584-0_5

[27] Wehrkamp-Richter T., Hinterhölzl R., Pinho S. T.: Damage and failure of triaxial braided composites under multi-axial stress states. Composites Science and Technology, **150**, 32–44 (2017).
https://doi.org/10.1016/j.compscitech.2017.07.002

[28] Ladevèze P., LeDantec E.: Damage modelling of the elementary ply for laminated composites. Composites Science and Technology, **43**, 257–267 (1992).
https://doi.org/10.1016/0266-3538(92)90097-M

[29] Casapu M., Fuiorea I., Arrigoni M.: Experimental characterization of internal structure and physical properties of unidirectional ply-level hybrid carbon composite material. Advanced Engineering Materials, in press, 2201447 (2023).
https://doi.org/10.1002/adem.202201447

[30] Merzkirch M., Foecke T.: 10° off-axis testing of CFRP using DIC: A study on strength, strain and modulus. Composites Part B: Engineering, **196**, 108062 (2020).
https://doi.org/10.1016/j.compositesb.2020.108062

[31] Goidescu C., Welemane H., Garnier C., Fazzini M., Brault R., Péronnet E., Mistou S.: Damage investigation in CFRP composites using full-field measurement techniques: Combination of digital image stereo-correlation, infrared thermography and X-ray tomography. Composites Part B: Engineering, **48**, 95–105 (2013).
https://doi.org/10.1016/j.compositesb.2012.11.016

[32] Fathi A., Keller J-H., Altstaedt V.: Full-field shear analyses of sandwich core materials using digital image correlation (DIC). Composites Part B: Engineering, **70**, 156–166 (2015).
https://doi.org/10.1016/j.compositesb.2014.10.045

[33] EN ISO 527-5:2009: Plastics. Determination of tensile properties. Test conditions for unidirectional fibre-reinforced plastic composites (2009).

[34] Liu B., Lessard L. B.: Fatique and damage-tolerance analysis of composite laminates: Stiffness loss, damage-modelling, and life prediction. Composites Science and Technology, **51**, 43–51 (1994).
https://doi.org/10.1016/0266-3538(94)90155-4

[35] Lemaître J., Chaboche J. L.: Mechanics of solid materials. Cambridge University Press, Cambridge (1990).

[36] Zhai Z., Jiang B., Drummer D.: Characterization of nonlinear response in quasi-unidirectional E-glass fabric reinforced polypropylene composites under off-axis tensile loading. Polymer Testing, **63**, 521–529 (2017).
https://doi.org/10.1016/j.polymertesting.2017.09.019

[37] O'Higgins R. M., McCarthy C. T., McCarthy M. A.: Identification of damage and plasticity parameters for continuum damage mechanics modelling of carbon and glass fibre-reinforced composite materials. Strain, **47**, 105–115 (2011).
https://doi.org/10.1111/J.1475-1305.2009.00649.X

[38] van Paepegem W., de Baere I., Degrieck J.: Modelling the nonlinear shear stress–strain response of glass fibre-reinforced composites. Part I: Experimental results. Composites Science and Technology, **66**, 1455–1464 (2006).
https://doi.org/10.1016/j.compscitech.2005.04.014

[39] Lafarie-Frenot M. C., Touchard F.: Comparative in-plane shear behaviour of long-carbon-fibre composites with thermoset or thermoplastic matrix. Composites Science and Technology, **52**, 417–425 (1994).
https://doi.org/10.1016/0266-3538(94)90176-7

[40] Fuller J. D., Wisnom M. R.: Ductility and pseudo-ductility of thin ply angle-ply CFRP laminates under quasi-static cyclic loading. Composites Part A: Applied Science and Manufacturing, **107**, 31–38 (2018).
https://doi.org/10.1016/j.compositesa.2017.12.020

[41] Fitoussi J., Meraghni F., Jendli Z., Hug G., Baptiste D.: Experimental methodology for high strain-rates tensile behaviour analysis of polymer matrix composites. Composites Science and Technology, **65**, 2174–2188 (2005).
https://doi.org/10.1016/j.compscitech.2005.05.001

[42] Wang J., Xiao Y., Inoue K., Kawai M., Xue Y.: Modeling of nonlinear response in loading-unloading tests for fibrous composites under tension and compression. Composites Structures, **207**, 894–908 (2019).
https://doi.org/10.1016/j.compstruct.2018.09.054

[43] Castres M., Berthe J., Deletombe E., Brieu M.: Étude du comportement non linéaire en cisaillement des CFRP : évaluation et modélisation de la limite élastique, étude de l'évolution de l'endommagement. CFM 2017 – 23ème Congrès Français de Mécanique, Aug 2017, Lille, France.
https://hal.science/hal-03465272

[44] Eliopoulos E. N., Philippidis T. P.: A progressive damage simulation algorithm for GFRP composites under cyclic loading. Part I: Material constitutive model. Composites Science and Technology, **71**, 742–749 (2011).
https://doi.org/10.1016/j.compscitech.2011.01.023

[45] Basaran C., Nie S.: An irreversible thermodynamics theory for damage mechanics of solids. International Journal of Damage Mechanics, **13**, 205–223 (2004).
https://doi.org/10.1177/1056789504041058

[46] Kawai M., Negishi R.: Micromechanical analysis for off-axis nonlinear behavior of unidirectional carbon fiber composite at room and high temperatures. Key Engineering Materials, **177–180**, 309–314 (2000).
https://doi.org/10.4028/www.scientific.net/kem.177-180.309

[47] Cheng L., Xiao Y., Wang J., Zhao J., Zhang Z., Xue Y.: Characterization and modeling of the ratcheting behavior of unidirectional off-axis composites. Composite Structures, **273**, 114305 (2021). https://doi.org/10.1016/j.compstruct.2021.114305

[48] Sinclair J. H., Chamis C. C.: Mechanical behavior and fracture characteristics of off-axis fiber composites I – experimental investigation. NASA, Cleveland (1977).

[49] Al-Hajaj Z., Sarwar A., Zdero R., Bougherara H.: *In-situ* damage assessment of a novel carbon/flax/epoxy hybrid composite under tensile and compressive loading. Journal of Composite Materials, **53**, 2701–2714 (2019). https://doi.org/10.1177/0021998319839129

[50] Machado R. D., Filho J. E. A., da Silva M. P.: Stiffness loss of laminated composite plates with distributed damage by the modified local Green's function method. Composite Structures, **84**, 220–227 (2008). https://doi.org/10.1016/j.compstruct.2007.08.001

[51] Zhao Y. Q., Zhou Y., Huang Z. M., Batra R. C.: Experimental and micromechanical investigation of T300/7901 unidirectional composite strength. Polymer Composites, **40**, 2639–2652 (2019). https://doi.org/10.1002/PC.25059